Crystal structure of $La_4Mg_3W_3O_{18}$ layered oxide

2005 J. Phys.: Condens. Matter 17 2585

(http://iopscience.iop.org/0953-8984/17/17/006)

INSTITUTE OF PHYSICS PUBLISHING JOURNAL OF PHYSICS: CONDENSED MATTER

J. Phys.: Condens. Matter **17** (2005) 2585–2595 doi:10.1088/0953-8984/17/17/006

Crystal structure of $La_4Mg_3W_3O_{18}$ layered oxide

D D Khalyavin, A M R Senos and P Q Mantas

Department of Ceramics and Glass Engineering, CICECO, University of Aveiro, 3810-193 Aveiro, Portugal

E-mail: dkhalyavin@cv.ua.pt, anamor@cv.ua.pt and pmantas@cv.ua.pt

Received 27 December 2004, in final form 11 March 2005
Published 15 April 2005
Online at stacks.iop.org/JPhysCM/17/2585

Abstract

The crystal structure of A-site deficient $La_4Mg_3W_3O_{18}$ perovskite has been solved by x-ray powder diffraction in combination with group theoretical analysis. Above 700 K, the crystal structure is orthorhombic (space group $Ibam$; $2a_p \times 4a_p \times 2a_p$ type superstructure) and presents a sequence of $[LaO]$–$[Mg_{1/2}W_{1/2}O_2]$–$[La_{1/3}O]'$–$[Mg_{1/2}W_{1/2}O_2]$–$[LaO]$–$[Mg_{1/2}W_{1/2}O_2]$–$[La_{1/3}O]''$–$[Mg_{1/2}W_{1/2}O_2]$ layers stacked along the b axis. The lanthanum ions and the vacancies in the $[La_{1/3}O]'$ and $[La_{1/3}O]''$ layers are ordered and form rows along the c axis. A half-period shift along the a direction between these layers leads to a quadrupling of the primitive perovskite unit cell in the b direction. The ordering of the vacancies in the lanthanum poor layers is connected with the ionic ordering between Mg^{2+} and W^{6+} in the neighbouring $[Mg_{1/2}W_{1/2}O_2]$ blocks. Around 700 K, due to an anti-phase rotation of the octahedra, a continuous phase transition mediated by the Γ_2^+ irreducible representation from orthorhombic ($Ibam$, $a^0b^0c^0$) to monoclinic ($C2/m$, $a^0b^0c^-$) symmetry takes place.

1. Introduction

Currently, a great number of crystal structures related to the perovskite one have been studied [1]. Among them, there can be distinguished compounds of which the crystal structure is obtained from the perovskite lattice by removing part of the cations or anions, i.e., perovskite structures containing cation/anion vacancies. From the crystal chemistry point of view, the compounds where cation/anion vacancies are ordered and form translational symmetry superstructures are of special interest. Very often, these compounds show interesting and useful properties. For example, the anion-deficient perovskites with ordered oxygen vacancies, $LnBa_2Cu_3O_{7+\delta}$ and $LnBaCo_2O_{5+\delta}$ (Ln = lanthanide), exhibit high temperature superconducting [2, 3] and giant magnetoresistance [4, 5] phenomena, respectively.

Another interesting example of vacancy ordering in perovskites is $La_{2/3}TiO_3$. This compound is unstable but it can be stabilized by small substitutions (∼10%) of La or Ti by other

cations (like Ni, Nb or Al substituting Ti or Sr substituting La). The crystal structure of this perovskite can be represented by a sequence of layers, [LaO]–[TiO_2]–[$La_{1/3}O$]–[TiO_2], stacked along the *c* axis [6, 7]. The alternation of the fully and partially occupied lanthanum-containing (001) planes forms a tetragonal superstructure of the type $a_p \times a_p \times 2a_p$ (a_p is the primitive perovskite unit cell). The compound and its solid solutions are widely investigated because of the intriguing microwave dielectric characteristics [8–10] and a considerable value of the ionic conductivity at high temperatures [11, 12]. However, in spite of the long history and of the great amount of work devoted to the investigation of this compound, only very recently has the room temperature crystal structure of $La_{2/3}TiO_3$ stabilized by 10% of Sr (LST) been adequately described by Howard and Zhang [13]. One of the problems in revealing some of the structural peculiarities, namely those connected with the rotation of the octahedra, is related to the need for a careful analysis of the data, which difficult to perform with the usual x-ray diffraction experiments. According to Howard and Zhang, the room temperature crystal structure of $La_{2/3}TiO_3$ is characterized by orthorhombic symmetry, space group *Cmmm*. The cation vacancies in the lanthanum-poor [$La_{1/3}O$] layers are distributed randomly and the orthorhombic distortions are caused by anti-phase rotation of the TiO_6 octahedra around the axis perpendicular to the direction of the cation ordering.

If the Ti^{4+} ions in $La_{2/3}TiO_3$ are substituted by a pair of ions, B′ and B″, with a strong difference in charge such that there appears an ionic ordering in the [$B'_{1-x}B''_xO_2$] layers, then this ordering can influence the distribution of the La^{3+} ions and vacancies in the neighbouring [$La_{1/3}O$] layers. An example of this kind of compound is $La_{2/3}Mg_{1/2}W_{1/2}O_3$($La_4Mg_3W_3O_{18}$), which was synthesized by Torii [14] more than 20 years ago. According to Torii, there is also a sequence of fully and partially occupied lanthanum-containing planes, and an NaCl-type ionic ordering between Mg^{2+} and W^{6+} is present in this compound. The intriguing fact is the presence of superstructure reflections pointing to a quadrupling of the primitive unit cell in one of the crystallographic directions, the nature of which Torii did not clarify. Therefore, the main goal of the present work is to reinvestigate the crystal structure of $La_4Mg_3W_3O_{18}$ (LMT), paying special attention to the distribution of the lanthanum ions and the vacancies in the [$La_{1/3}O$] layers and the possible lowering of the symmetry due to the tilting of the octahedra.

2. Experimental details

To prepare the $La_4Mg_3W_3O_{18}$ (LMT) oxide, powders of La_2O_3 (99.5%, Merck), MgO (98%, Fluka) and WO_3 (99.9% Fluka) were weighed according to the stoichiometry of the composition and mixed for 4 h, in a polyethylene container with ethanol and zirconia balls, in a planetary mill. The slurries were dried in an oven at 120 °C and the dried powders were deagglomerated. The powders were then calcined at 1200 °C for 4 h. After calcination, the materials were deagglomerated again. Finally, pellets with 10 mm diameter and 5–6 mm height were obtained by uniaxial pressing in a steel die under 60 MPa, followed by an isostatic pressing at 200 MPa. The pellets were sintered in air for 6 h at 1300, 1350, 1400 and 1450 °C. The heating and cooling rates were 100 °C h^{-1}. Weight losses during the sintering did not exceed 1.5%. The microstructure of the sintered specimens was characterized by scanning electron microscopy (SEM, Hitachi S-4100).

To obtain powders for x-ray diffraction experiments the sintered pellets were crushed in an agate mortar. The room temperature x-ray powder diffraction data were collected using a Rigaku D/MAX-B diffractometer (Cu Kα radiation; tube power 40 kV, 30 mA; 2θ range 10°–120°, step 0.02°, 20 s/step; graphite monochromator; receiving slit 0.15 mm). The high temperature x-ray diffraction experiments were carried out on a Philips X'Pert MPD

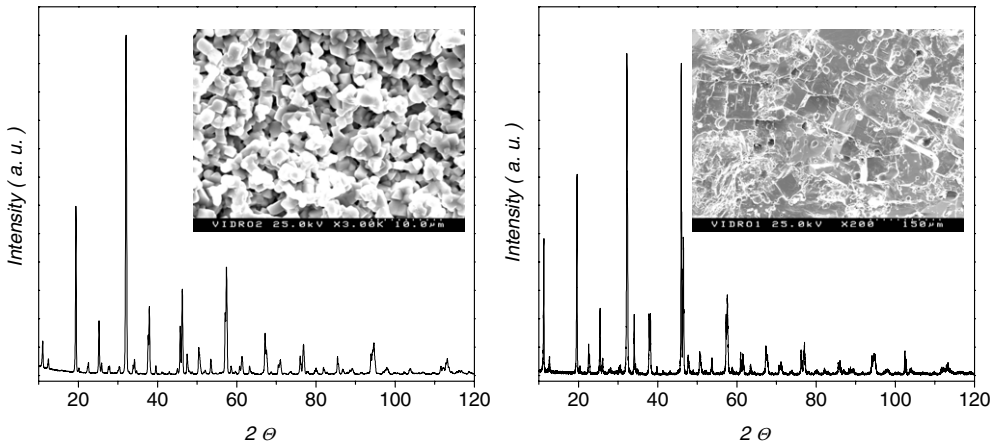

Figure 1. X-ray powder diffraction patterns of $La_4Mg_3W_3O_{18}$ perovskite sintered at 1300 °C (left panel) and 1400 °C (right panel). The insets show the SEM observations of the corresponding microstructure.

diffractometer (Cu Kα radiation; tube power 40 kV, 30 mA; graphite monochromator). The full spectrum was recorded at 900 K (2θ range 10°–120°, step 0.02°, 5 s/step; receiving slit 0.15 mm), whereas at intermediate temperatures only selected reflections were examined (step 0.01°, 30 s/step; receiving slit 0.05 mm). The obtained data were refined by the Rietveld method using the Fullprof program [15] and assuming a pseudo-Voigt profile shape function. The background was described by interpolation of selected points. A small amount of $La_2W_{1.25}O_{6.75}$ (card No 32-0503 PDF) impurity phase (strongest line $\sim$1%) was detected. Since we did not find a description of the crystal structure of this compound in the literature to introduce it as a second phase into the calculations, the parts of the spectra where the impurity peaks did not overlap with the general phase were removed from the refinement procedure.

3. Results and discussion

Room temperature XRD patterns of LMW sintered at different temperatures are presented in figure 1. It is observed that the intensity of some of the reflections increases significantly when the sintering temperature increases. This points to an appearance of preferred orientation due to an anisotropic development of the grains (crystals), a situation that is indeed revealed by the microstructures (see the insets in figure 1): in the sample sintered at 1400 °C, figure 1(b), anisotropic grain growth is clearly observed, with grains of rectangular shape reaching very large lengths, $\sim$200 μm. A more careful analysis of these microstructures indicates that the sintering process, above 1400 °C, probably occurs in the presence of a liquid phase. If this is the case, then LMW melts incongruently. Since, for the samples sintered at $T \geqslant 1400$ °C, the intensities of the XRD peaks reflect the development of the preferred orientation, the analysis of the crystal structure will be done with the spectra of the samples sintered below that temperature.

The analysis of the LMW spectra will be performed in the frame of the perovskite type crystal structure. We will present the work in the following two ways:

(i) we will start with the analysis of the room temperature spectrum to clarify the cation distribution and to propose a basic model for the crystal structure of LMW; then,

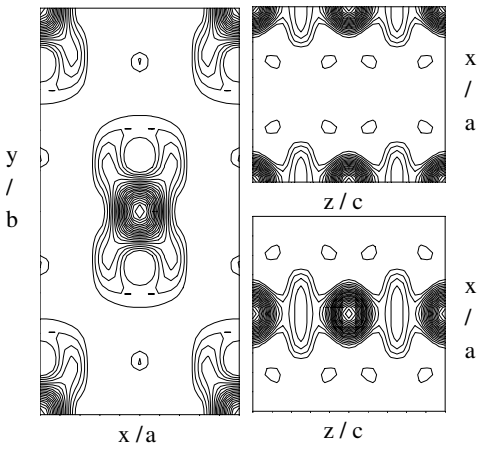

Figure 2. Harker sections of the Patterson function based on the superstructure reflections: left section, $z = 0$; right, upper section, $y = 0$; and right, lower section $y = 0.5$.

(ii) we will show the XRD spectra at different temperatures, allowing the conclusion that the proposed crystal structure is only valid for high temperatures, whereas the crystal structure at room temperature includes a rotation of the oxygen octahedra.

3.1. Analysis of the room temperature spectrum

Figure 1(a) presents the spectrum under analysis. A set of reflections corresponding to the fundamental multiplets of the aristotype perovskite structure can be distinguished. The splitting of some of these (hkl) reflections into triplets when $h = k \neq l$, and the non-splitting of the reflections when $h = k = l$, are both consistent with the orthorhombic metric of the primitive perovskite unit cell. We have chosen the setting where $b_p > c_p > a_p$. The presence of strong superstructure reflections of the $(h + \frac{1}{2}\, k + \frac{1}{2}\, l + \frac{1}{2})$ type shows evidence of the ordering between Mg^{2+} and W^{6+}, of the NaCl type, and that of the $(hk + \frac{1}{2}\, l)$ type indicates an alternation of the occupancy of the lanthanum-containing planes, fully–partially–fully occupied, along the b direction, analogously to the situation occurring in $La_{2/3}TiO_3$ [6, 7]. However, a successful indexation of the spectrum involves the quadrupling of the primitive unit cell in the b direction and, since the intensities of the corresponding superstructure reflections are rather strong, that procedure is quite probably associated with the distribution of the cations.

The most probable reason to have the quadrupling of the unit cell comes from the ordering of the lanthanum ions and vacant sites of the partially occupied La-containing planes. To clarify the distribution of the lanthanum ions in these layers, we have calculated the Patterson function, $P(x, y, z)$, using the superstructure reflections,

$$P(x, y, z) = \sum_h \sum_k \sum_l |F_{hkl}|^2 \cos[2\pi(hx + ky + lz)] \tag{1}$$

where $|F_{hkl}|$ is the structural amplitude of the hkl superstructure reflection. These amplitudes were taken from the La Bail fitting [16] of the XRD spectrum, using the $Pmmm$ space group, which does not contain absence conditions, and the $2a_p \times 4b_p \times 2c_p$ unit cell. Figure 2 shows the Harker sections of the Patterson function based on 12 superstructure reflections and on the $Pmmm$ space group. Four general maxima can be observed with equivalent densities, at coordinates $x_j y_j z_j = 000$, $00\frac{1}{2}$, $\frac{1}{2}\,\frac{1}{2}0$ and $\frac{1}{2}\,\frac{1}{2}\,\frac{1}{2}$. This is the case when coordinates of the density maxima of the Patterson function coincide with the positions of the atoms in the

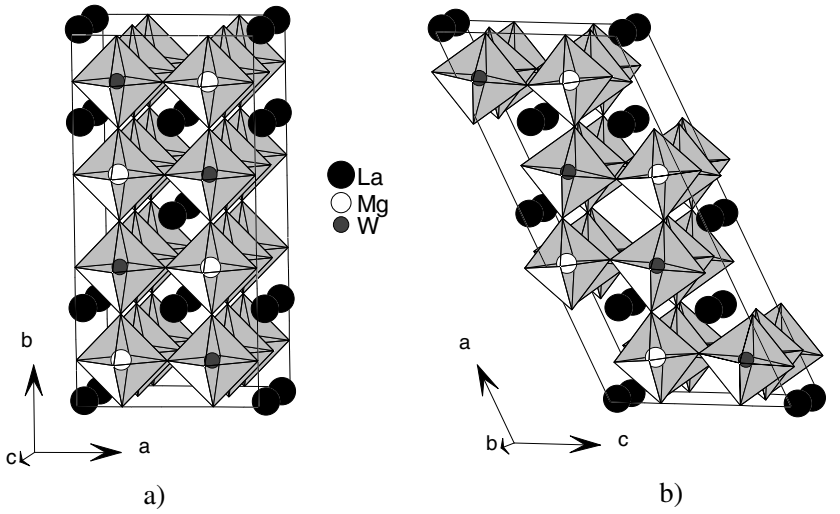

Figure 3. Schematic representation of the crystal structure of $La_4Mg_3W_3O_{18}$ above 700 K (a), and below 700 K (b).

supercell. Indeed, the superstructure reflections originating from this superlattice satisfy both $h + k + l = 2n$ (body centred) and $h + k = 2n$ (face centred) absence rules, which means that the $2\pi(hx_j + ky_j + lz_j)$ phase term always equals $2\pi n$ and, therefore, the coordinates of the $P(x, y, z)$ peaks are coincident with the peak positions of the inverse Fourier transform, $F(x, y, z)$,

$$F(x, y, z) = \sum_h \sum_k \sum_l F_{hkl} \exp\{-2\pi \mathrm{i}(hx + ky + lz)\} \tag{2}$$

representing the maxima of the electronic density of the unit cell. Thus, the maxima in figure 2 are easily assigned to the position of the lanthanum ions.

We finally arrive at the basic model for LMW at this point (figure 3(a)). It is characterized by the orthorhombic *Ibam* space group and implies a sequence of layers stacked along the *b* axis: [LaO]–[$Mg_{1/2}W_{1/2}O_2$]–[$La_{1/2}O]'$–[$Mg_{1/2}W_{1/2}O_2$]–[LaO]–[$Mg_{1/2}W_{1/2}O_2$]–[$La_{1/2}O]''$–[$Mg_{1/2}W_{1/2}O_2$]. The lanthanum ions and the vacant sites in the 'lanthanum-deficient' layers, [$La_{1/2}O]'$ and [$La_{1/2}O]''$, form rows along the *c* direction and there is a half-period shift in the *a* direction giving rise to the quadrupling of the primitive unit cell along the *b* direction (the $2a_p \times 4a_p \times a_p$ type superstructure). The proposed model corresponds to an $La_3Mg_2W^{5+}W^{6+}O_{12}$ chemical formula assuming a full occupancy of all the atomic positions. Therefore, the $La_4Mg_3W_3O_{18}$ chemical composition suggests the presence of vacant sites in the lanthanum positions. The lanthanum ions occupy two different positions in the *Ibam* space group: $4a$, in the [$La_{1/2}O]'$/[$La_{1/2}O]''$ layers, and $8g$, in the [LaO] layers. The refinement procedure allows us to conclude that the vacant sites are almost entirely located in the $4a$ position, which means that, actually, the sequence of [LaO]–[$Mg_{1/2}W_{1/2}O_2$]–[$La_{1/3}O]'$–[$Mg_{1/2}W_{1/2}O_2$]–[LaO]–[$Mg_{1/2}W_{1/2}O_2$]–[$La_{1/3}O]''$–[$Mg_{1/2}W_{1/2}O_2$] layers takes place.

3.2. Analysis at higher temperatures

In this section we analyse the temperature behaviour of the unit cell parameters of the proposed crystal structure, in an analogous way to that performed for $La_{0.6}Sr_{0.1}TiO_3$ (LST) [13].

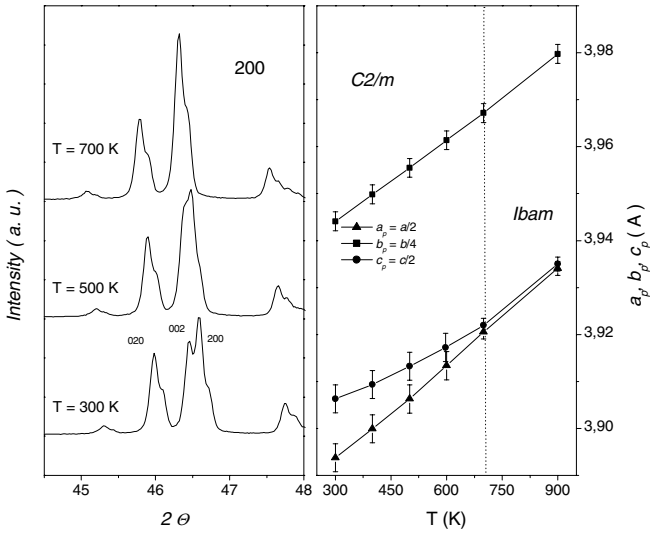

Figure 4. Temperature evolution of the 200 fundamental multiplet (left panel) and the primitive perovskite translations (right panel).

This compound presents a phase transition at ∼640 K associated with an anti-phase tilting of the TiO_6 octahedra and, since the compound is closely related to LMW, it is conceivable that LMW also presents a rotation of the equivalent octahedra, $(Mg/W)O_6$. However, it should be noted that in our case the analysis of the superstructure reflections associated with anti-phase octahedral tilting $(h+\frac{1}{2}\ k+\frac{1}{2}\ l+\frac{1}{2})$ is complicated by the much larger contribution to structural factors of these reflections coming from the ionic ordering between Mg^{2+} and W^{6+}.

Figure 4 shows the temperature evolution of the 200 fundamental multiplet and of the parameters of the primitive unit cell. Upon increasing the temperature, a_p and c_p approach each other and practically merge together (the difference between them is smaller than the resolution of the apparatus) at ∼700 K. Above this temperature only changes associated with the thermal expansion occur. This behaviour suggests a continuous phase transition at 700 K, a phase transition associated with the rotation of the octahedra. Therefore, the model of the crystal structure presented in the previous section is not adequate for temperatures below 700 K, but it is for higher temperatures: table 1 presents the results of the refinements, with the *Ibam* space group, of the XRD spectrum recorded at 900 K. The very close values of the a_p and c_p parameters in the high temperature orthorhombic phase are caused by the fact that along these directions the alternation of the planes equivalently occupied by lanthanum ions takes place. For comparison, along the [010] direction, the sequence $1–\frac{1}{3}–1–\frac{1}{3}–1\ldots$ (1—fully occupied and $\frac{1}{3}$—one third occupied lanthanum-containing planes) occurs, whereas along both the [100] and the [001] directions, the sequence is $\frac{2}{3}–\frac{2}{3}–\frac{2}{3}–\frac{2}{3}\ldots$. ($\frac{2}{3}$—two thirds occupied planes) (see figure 3(a)).

3.3. Group-theoretical analysis

The low temperature crystal structure is inferred from the tilting of the octahedra of the *Ibam* structure. Group theoretical analysis will be used with Landau's constraint for allowed continuous phase transitions. To do that we will apply the methodology proposed by Howard and Stokes [17] and the capabilities of the computer program ISOTROPY [17, 18]. To identify the basic components of the tilted systems (anti-phase or in-phase rotation of the octahedra

Table 1. Atomic coordinates and isotropic thermal parameters (B_{iso}) for $La_4Mg_3W_3O_{18}$ at 900 K. Space group $Ibam$, cell parameters: $a = 7.8682(10)$ Å, $b = 15.9230(10)$ Å, $c = 7.8700(10)$ Å, $V = 986.00(19)$ Å^3; $Z = 16$. Reliability factors: $R_p = 6.96\%$, $R_{wp} = 9.88\%$.

Atom	Position	Occupation	x	y	z	B_{iso} (Å^2)
La1	4a	0.521(5)	0	0	0.25	1.29(6)
La2	8g	0.951(8)	0	0.2477(2)	0.25	1.29(6)
La3	4b	0.059(4)	0.5	0	0.25	1.29(6)
Mg1	8j	1	−0.2602(25)	−0.1213(5)	0	1.97(28)
W1	8j	0.949(8)	0.2561(3)	−0.1185(1)	0	0.56(4)
O1	8j	1	−0.0108(42)	−0.1497(11)	0	2.63(16)
O2	8j	1	−0.0062(51)	−0.3631(11)	0	2.63(16)
O3	8j	1	−0.2226(21)	0.0039(10)	0	2.63(16)
O4	8j	1	−0.2845(27)	0.2499(10)	0	2.63(16)
O5	16k	1	0.2705(15)	0.3785(10)	0.2416(21)	2.63(16)

Table 2. The tilt system, irreducible representation, space group symmetry (and number), lattice vectors and the origin of the subgroup with respect to the parent cell in $Ibam$.

Tilt system	Irred. rep.	Space group	Lattice vectors	Origin
$a^0b^0c^0$	Γ_1^+	$Ibam$ (No. 72)	(1, 0, 0) (0, 1, 0) (0, 0, 1)	(0, 0, 0)
$a^+b^0c^0$	X_1^-	$Pban$ (No. 50)	(1, 0, 0) (0, 1, 0) (0, 0, 1)	$(\frac{1}{4}, \frac{1}{4}, \frac{1}{4})$
$a^0b^+c^0$	Γ_1^-	$I222$ (No. 23)	(1, 0, 0) (0, 1, 0) (0, 0, 1)	$(0, 0, \frac{1}{4})$
$a^0b^0c^+$	X_1^+	$Pccm$ (No. 49)	(1, 0, 0) (0, 1, 0) (0, 0, 1)	(0, 0, 0)
$a^-b^0c^0$	Γ_3^+	$C2/c$ (No. 15)	(0, 1, 1) (1, 0, 0) (0, 0, −1)	(0, 0, 0)
$a^0b^-c^0$	Γ_4^+	$C2/c$ (No. 15)	(1, 0, −1) (0, 1, 0) (0, 0, 1)	(0, 0, 0)
$a^0b^0c^-$	Γ_2^+	$C2/m$ (No. 12)	(−1, 1, 0) (0, 0, 1) (1, 0, 0)	(0, 0, 0)

around one of the directions [100], [010] or [001]), which form a set of basis functions, we will use Glazer's notation [19].

The $Ibam$ space group does not contain elements that mix the basis functions and, therefore, the irreducible representations transforming them are one-dimensional. Following the soft mode concept, this means that the phase transition at 700 K only involves the rotation of the octahedra around one of the crystallographic axis, i.e., it is enough to consider only one-tilted structures. To find the irreducible representations for which the basic components of tilt systems are basis functions, all possible distortions caused by the pseudovectors at the Wyckoff position j were generated by the program ISOTROPY, taking into consideration the irreducible representations at the κ points of symmetry. The inspection of the distortions produced by the one-dimensional irreducible representations allowed us to identify X_1^-, Γ_1^-, X_1^+, Γ_3^+, Γ_4^+ and Γ_2^+ (in the notation of Miller and Love [20]) with the $a^+b^0c^0$, $a^0b^+c^0$, $a^0b^0c^+$, $a^-b^0c^0$, $a^0b^-c^0$ and $a^0b^0c^-$ tilted systems, respectively. The corresponding isotropy subgroups are $Pban$, $I222$, $Pccm$, $C2/c$, $C2/c$ and $C2/m$. In all cases, the phase transitions are allowed to be continuous by Landau theory. Table 2 lists all of these space groups and the corresponding irreducible representations and tilted systems, together with the lattice vectors and the origin of the subgroups. The isotropy subgroup for any of the two- or three-tilted system can be found by considering the reducible representation which is obtained as a direct sum of the corresponding two or three above-mentioned irreducible representations. The results described above can be obtained from a 'first principles' group-theoretical approach, detailed in the appendix.

Applying now the two conditions, continuity of the phase transition and $c_p > a_p$, we can infer the symmetry of LMW below 700 K. Both conditions are satisfied by the $a^0b^0c^+$ and $a^0b^0c^-$ tilted systems, but for the first case there is expected to be the presence of $(h+\frac{1}{2}\,k+\frac{1}{2}\,l)$,

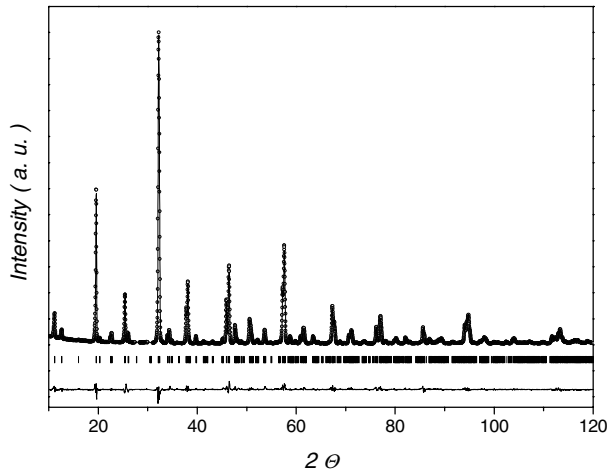

Figure 5. Observed (circles), calculated (continuous curve) and difference (solid line below the spectrum) room temperature x-ray powder diffraction pattern of $La_4Mg_3W_3O_{18}$. The vertical bars correspond to the calculated peak positions.

Table 3. Atomic coordinates and isotropic thermal parameters (B_{iso}) for $La_4Mg_3W_3O_{18}$ at room temperature. Space group $C2/m$, cell parameters: $a = 17.6454(10)$ Å, $b = 7.8335(10)$ Å, $c = 7.8155(10)$ Å, $\beta = 116.36(1)^\circ$, $V = 967.97(18)$ Å^3; $Z = 16$. Reliability factors: $R_p = 6.30\%$, $R_{wp} = 8.83\%$.

Atom	Position	Occupation	x	y	z	B_{iso} (Å^2)
La1	4g	0.552(6)	0	0.2559(19)	0	0.29(3)
La2	8j	0.942(9)	0.2480(2)	0.2503(9)	0.2508(8)	0.29(3)
La3	4h	0.027(2)	0.2498(4)	0.5	0.25	0.29(3)
Mg1	4i	1	−0.1204(17)	0	−0.3921(41)	0.38(21)
Mg2	4i	1	0.6204(17)	0	−0.1421(41)	0.38(21)
W1	4i	0.934(8)	−0.1191(4)	0	0.1298(8)	0.15(2)
W2	4i	0.934(8)	0.6191(3)	0	0.3798(8)	0.15(2)
O1	4i	1	0.6311(25)	0	−0.1772(51)	0.84(16)
O2	4i	1	−0.0062(51)	0	0.1405(62)	0.84(16)
O3	4i	1	−0.3482(26)	0	−0.3692(57)	0.84(16)
O4	4i	1	0.9011(18)	0	0.3926(56)	0.84(16)
O5	4i	1	0.0136(19)	0	−0.1594(35)	0.84(16)
O6	4i	1	0.4983(14)	0	−0.2491(49)	0.84(16)
O7	4i	1	−0.2492(26)	0	−0.5574(61)	0.84(16)
O8	4i	1	0.7544(22)	0	−0.0222(67)	0.84(16)
O9	8j	1	0.3874(12)	0.2347(28)	0.7026(27)	0.84(16)
O10	8j	1	−0.3627(16)	0.2654(28)	−0.1227(35)	0.84(16)

with $h \neq k$, superstructure reflections. They were not observed in the room temperature XRD spectrum and, therefore, this spectrum was refined using the monoclinic $C2/m$ space group (figure 5). The crystallographic parameters obtained in this refinement are listed in table 3, and a schematic representation of the crystal structure is shown in figure 3(b).

3.4. Further considerations

It was shown above that LMW 'needs' a quadrupling of the unit cell to be characterized. This is because the vacant sites of the $[La_{1/2}O]$ layers are not randomly distributed, like in the case

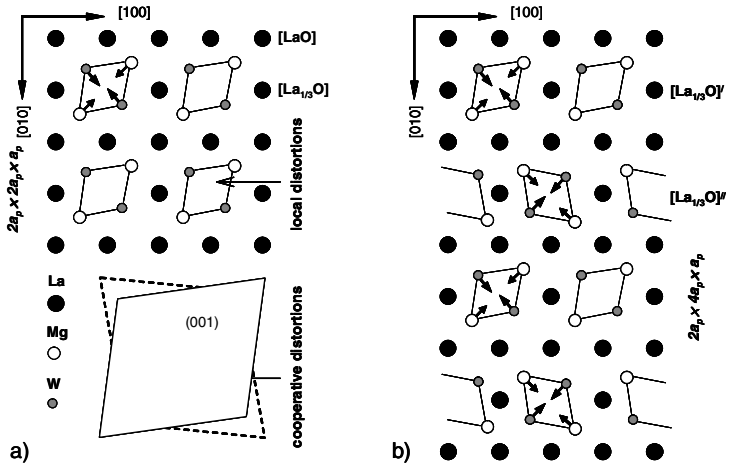

Figure 6. Schematic representation of the magnesium/tungsten cation displacements within (001) planes in the cases of $2a_p \times 2a_p \times a_p$ (a) and $2a_p \times 4a_p \times a_p$ (b) superstructures.

of LST [13], but ordered. The stacking of these $[La_{1/2}O]$ layers along the b direction could also be of the $2a_p \times 2a_p \times a_p$ type, instead of the $2a_p \times 4a_p \times a_p$ one, still presenting an ordering of the vacant sites, but only needing a doubling of the unit cell (figure 6(a)). However, in this case the elastic energy of the lattice would be higher than that when a quadruple unit cell is present. This is due to the displacement of the Mg and W ions in the (001) planes towards the $[La_{1/2}O]$ layers, with components in the $[100]/[\bar{1}00]$ and $[010]/[0\bar{1}0]$ directions. These displacements are different, because there is a large difference in the charge and in the size of the cations involved (see in figure 6(a) the resulting lozenge of these displacements). In the case of the doubling of the unit cell, the W ions are always displaced along the $[110]/[\bar{1}\bar{1}0]$ directions and the Mg ions along the $[1\bar{1}0]/[\bar{1}10]$ ones within the same (001) plane. In the neighbouring (001) planes the character of the displacement of the atoms is the opposite one: the W ions are always displaced along $[1\bar{1}0]/[\bar{1}10]$ and the Mg ions along $[110]/[\bar{1}\bar{1}0]$. The cooperative character of these distortions in the whole (001) plane (all the lozenges are in the same position) is lightened if, instead, alternatively the W ions are displaced along the $[110]/[\bar{1}\bar{1}0]$ and $[1\bar{1}0]/[\bar{1}10]$ directions and the Mg ions in the $[1\bar{1}0]/[\bar{1}10]$ and $[110]/[\bar{1}\bar{1}0]$ directions (the lozenges would be in alternative positions, as seen in figure 6(b)). Therefore, the quadrupling of the unit cell structure is energetically more stable than the doubling one.

The displacements of magnesium and tungsten ions described above in combination with the row-type ordering of lanthanum ions and vacancies in the $[La_{1/3}O]'$ and $[La_{1/3}O]''$ layers lead to effective compensation of the deficiency of positive charge in these layers. The additional localization of vacancies into the rows, in comparison with $La_{2/3}TiO_3$, where lanthanum ions and vacancies are distributed randomly within the lanthanum poor layers, is possible due to the cation ordering between Mg^{2+} and W^{6+} ions, which results in a smaller electrostatic repulsion of the shifted cations. Possible implications of these characteristics of the LMW crystal structure on, for example, the electrical properties of the compound are beyond the scope of the present work, but will be treated in a forthcoming paper.

4. Conclusions

The crystal structure of $La_4Mg_3W_3O_{18}$ oxide is found to be closely related to the structure of $La_{2/3}TiO_3$, with the additional ordering of the lanthanum ions in the rows within the lanthanum-

poor layers and rock salt type cation ordering between magnesium and tungsten ($2a_p \times 4a_p \times 2a_p$ type superstructure). At temperatures higher than 700 K the symmetry is orthorhombic $Ibam$. Below this temperature the symmetry is lowered to monoclinic $C2/m$ as a result of a continuous phase transformation involving an anti-phase rotation of the octahedra around the axis parallel to the lanthanum-formed rows.

Acknowledgment

We wish to thank the Foundation for Science and Technology (FCT, Portugal) for financial support through grant SFRH/BPD/12669/2003.

Appendix

The 'first principles' approach for a group-theoretical analysis of the crystal structures, which can be derived from the crystal structure shown in figure 3(a), due to rotations of the octahedra, involves the irreducible representations of $Pm\bar{3}m$ space group for the calculations. According to Howard and Stokes [17], in-phase and anti-phase rotations of the octahedra around ⟨001⟩ axes of space group $Pm\bar{3}m$ are transformed as pseudovector basis functions of M_3^+ ($k = \frac{1}{2}, \frac{1}{2}, 0$) and R_4^+ ($k = \frac{1}{2}, \frac{1}{2}, \frac{1}{2}$) three-dimensional irreducible representations, respectively. The rock salt type cation ordering in the B-site position is described by an R_1^+ one-dimensional representation of $Pm\bar{3}m$ [21]. The ordering of lanthanum ions in the $[La_{1/3}O]'$ and $[La_{1/3}O]''$ layers, found in this work, can be associated with the Z_4 ($k = \frac{1}{4}, \frac{1}{2}, 0$) twelve-dimensional irreducible representation with the P2 ($a, 0, 0, 0, 0, 0, 0, 0, 0, 0, 0, 0$) direction of the order parameter in the representation space. By combining the $R_1^+ \oplus Z_4$ representation with the M_3^+ or/and R_4^+ ones, one can obtain, with the aid of ISOTROPY, a list of the isotropy subgroups, corresponding to the coupled order parameter. For example, the calculation of the isotropy subgroups for the $M_3^+/R_4^+ \oplus R_1^+ \oplus Z_4$ combinations gives $Pccm/C2/m$ space groups with the ($a, 0, 0, b, c, 0, 0, 0, 0, 0, 0, 0, 0, 0, 0, 0$) order parameter. A nonzero first component in the M_3^+/R_4^+ subspace corresponds to in-phase/anti-phase octahedral tilting around the z axis of space group $Pm\bar{3}m$. A nonzero second component in the $R_1^+ \oplus Z_4$ subspace indicates that the first distinct domain of $Ibam$, with the $(E|0, 0, 0)$ generator, is under consideration. In this domain, the lattice vectors of space group $Ibam$ are collinear with the corresponding lattice vectors of the $Pm\bar{3}m$ one ((4, 0, 0)(0, 2, 0)(0, 0, 2)), and therefore the $Pccm$ and $C2/m$ space groups should be associated with $a^0b^0c^+$ and $a^0b^0c^-$ tilt systems, respectively.

Further, $Pban$ and $I222$ isotropy subgroups, obtained in the frame of the first consideration for the $a^+b^0c^0$ and $a^0b^+c^0$ tilt systems, appear in the first principles calculation ($M_3^+ \oplus R_1^+ \oplus Z_4$ combination) with the ($a, 0, 0, b, 0, 0, 0, 0, 0, -c, 0, 0, 0, 0, 0, 0$) and the ($a, 0, 0, b, 0, 0, -c, 0, 0, 0, 0, 0, 0, 0, d, 0$) order parameters, respectively. The ($b, 0, 0, 0, 0, 0, -c, 0, 0, 0, 0, 0, 0, 0$) direction in the $R_1^+ \oplus Z_4$ subspace shows that the third distinct domain of $Ibam$, with the $(C_3^+|0, 0, 0)$ generator, is under consideration. In this domain, the lattice vectors of the $Ibam$ space group are (0, 4, 0)(0, 0, 2)(2, 0, 0) in respect to the parent $Pm\bar{3}m$ one. Therefore, the $Pban$ space group should be associated with the $a^0b^+c^0$ tilt system[1]. In the case of space group $I222$, the order parameter has two nonzero components in the Z_4 subspace. If one makes the d component 0, the direction of the order parameter in the $R_1^+ \oplus Z_4$ subspace will coincide with the order parameter in the second distinct domain,

[1] In the first consideration we used the $Ibam$ space group with quadrupling along the b axis, but here the a axis is the quadrupled one. Therefore the space groups, corresponding to the $a^{+/-}b^0c^0$ and $a^0b^{+/-}c^0$ tilt systems in the first consideration, correspond now to $a^0b^{+/-}c^0$ and $a^{+/-}b^0c^0$ tilt systems, respectively.

with the $(C_3^-|0, 0, 0)$ generator, which changes the z axis into the x axis ((0, 0, 4)(2, 0, 0)(0, 2, 0)). Thus, space group $I222$ corresponds to the $a^+b^0c^0$ tilt system. However, the given space group allows the ordering of La ions in the $[La_{1/2}O]'$ and $[La_{1/2}O]''$ layers to be more general (less symmetric) than the one shown in figure 3(a). This is the reason why the d component can be nonzero (in other words, a deviation of the d component from 0 does not change the symmetry). A similar situation has been recently discussed by Howard and Stokes [22] for octahedral tilting in $A_4B'B''_3X_{12}$ ordered perovskites.

A similar consideration of the $R_4^+ \oplus R_1^+ \oplus Z_4$ isotropy subgroups gives space group $C2/c$ with $(a, 0, 0, b, 0, 0, 0, 0, 0, -c, 0, 0, 0, 0, 0, 0)$ order parameter for the $a^0b^-c^0$ tilt system and space group[2] $C2/c$ with $(a, 0, 0, b, 0, 0, -c, 0, 0, 0, 0, 0, 0, 0, 0, d)$ order parameter for the $a^-b^0c^0$ tilt system, which again is entirely consistent with the previous analysis.

References

[1] Mitchell R H 2002 *Perovskites: Modern and Ancient* (Thunder Bay, ON: Almaz Press)
[2] Blatter G, Feigelman M V, Geshkenbein V B, Larkin A I and Vinokur V M 1994 *Rev. Mod. Phys.* **66** 1125
[3] MacManus Driscoll J L 1997 *Adv. Mater.* **9** 457
[4] Martin C, Maignan A, Pelloquin D, Nguyen N and Raveau B 1997 *Appl. Phys. Lett.* **71** 1421
[5] Troyanchuk I O, Kasper N V, Khalyavin D D, Szymczak H, Szymczak R and Baran M 1998 *Phys. Rev. Lett.* **80** 3380
[6] Abe M and Uchino K 1974 *Mater. Res. Bull.* **9** 147
[7] Bouwma J, de Vries K J and Burggraaf A 1976 *Phys. Status Solidi* a **35** 281
[8] Moon J H, Park H S, Lee K T, Choi J H, Yeo D H, Yoon S J and Kim H J 1997 *Japan. J. Appl. Phys.* **36** 6814
[9] Lee H J, Park H M, Cho Y K and Nahm S 2003 *J. Am. Ceram. Soc.* **86** 1395
[10] Salak A N, Seabra M P and Ferreira V M 2003 *J. Eur. Ceram. Soc.* **23** 2409
[11] Yashioka H and Kikkawa S 1998 *J. Mater. Chem.* **8** 1821
[12] Yashima M, Ali R and Yashioka H 2000 *Solid State Ion.* **128** 105
[13] Howard C J and Zhang Z 2003 *J. Phys.: Condens. Matter* **15** 4543
[14] Torii Y 1979 *Chem. Lett.* **10** 1215
[15] Rodriguez-Carvajal J 1993 *Physica* B **192** 55
[16] Le Bail A, Duroy H and Fourquet J L 1988 *Mater. Res. Bull.* **23** 447
[17] Howard C J and Stokes H T 1998 *Acta Crystallogr.* B **54** 782
[18] Stokes H T and Hatch D M 2002 *ISOTROPY* http://stokes.byu.edu/isotropy.html
[19] Glazer A M 1972 *Acta Crystallogr.* B **28** 3384
[20] Miller S C and Love W F 1967 *Tables of Irreducible Representations of Space Groups and Co-Representations of Magnetic Space Groups* (Boulder, CO: Preutt)
[21] Howard C J, Kennedy B J and Woodward P M 2003 *Acta Crystallogr.* B **59** 463
[22] Howard C J and Stokes H T 2004 *Acta Crystallogr.* B **60** 674

[2] These two $C2/c$ space groups are different in respect of the translational symmetry.